Functional network integration of embryonic stem cell-derived astrocytes in hippocampal slice cultures

Björn Scheffler[1,*], Tanja Schmandt[1,2], Wolfgang Schröder[3], Barbara Steinfarz[1,2], Leila Husseini[3], Jörg Wellmer[4], Gerald Seifert[3], Khalad Karram[1,2], Heinz Beck[4], Ingmar Blümcke[1], Otmar D. Wiestler[1], Christian Steinhäuser[3] and Oliver Brüstle[1,2,†]

[1]Department of Neuropathology, University of Bonn Medical Center, Sigmund-Freud-Strasse 25, D-53105 Bonn, Germany
[2]Institute of Reconstructive Neurobiology, University of Bonn Medical Center, Sigmund-Freud-Strasse 25, D-53105 Bonn, Germany
[3]Department of Neurosurgery, University of Bonn Medical Center, Sigmund-Freud-Strasse 25, D-53105 Bonn, Germany
[4]Department of Epileptology, University of Bonn Medical Center, Sigmund-Freud-Strasse 25, D-53105 Bonn, Germany
*Present address: Department of Neuroscience, Brain Institute, University of Florida, PO Box 100244, Gainesville, FL 32610-0244, USA
[†]Author for correspondence (e-mail: brustle@uni-bonn.de)

Accepted 9 July 2003

Development 130, 5533-5541

doi:10.1242/dev.00714

Summary

Embryonic stem (ES) cells provide attractive prospects for neural transplantation. So far, grafting strategies in the CNS have focused mainly on neuronal replacement. Employing a slice culture model, we found that ES cell-derived glial precursors (ESGPs) possess a remarkable capacity to integrate into the host glial network. Following deposition on the surface of hippocampal slices, ESGPs actively migrate into the recipient tissue and establish extensive cell-cell contacts with recipient glia. Gap junction-mediated coupling between donor and host astrocytes permits widespread delivery of dye from single donor cells. During maturation, engrafted donor cells display morphological, immunochemical and electrophysiological properties that are characteristic of differentiating native glia. Our findings provide the first evidence of functional integration of grafted astrocytes, and depict glial network integration as a potential route for widespread transcellular delivery of small molecules to the CNS.

Supplemental data available online

Key words: ES cells, Glia, Electrophysiology, Gap junction, Hippocampus, Slice culture

Introduction

The availability of embryonic stem cells offers exceptional opportunities for combining cell and gene therapy. Whereas in vitro differentiation of ES cells permits the generation of virtually unlimited numbers of donor cells for a large variety of tissues (Svendsen and Smith, 1999), homologous recombination and gene targeting can be exploited to tailor these cells to their individual application (Zimmer 1992). Recently, we developed a protocol for the derivation of highly purified ES cell-derived glial precursors. In vitro, these precursors give rise to both astrocytes and oligodendrocytes. Transplantation of ES cell-derived oligodendrocytes has been used successfully for myelin repair (Brüstle et al., 1999). In contrast to myelinating grafts, astrocyte transplantation has received little attention (Gates et al., 1998; Zhou and Lund, 1993). This is surprising considering the important functions of astrocytes in neuronal maintenance and stabilization of the extracellular milieu. Recent data on astrocyte-induced neurogenesis from adult neural stem cells further support the view that glial cells play an active rather than passive role in maintaining the neuronal population (Song et al., 2002).

In vivo, astrocytes are connected via gap junctions and form extensive networks (Giaume and McCarthy, 1996). Incorporation of transplanted ES cell-derived astrocytes into such a network structure could provide new perspectives for both cell-mediated delivery of small molecules and modulation of neuronal function. Despite these attractive prospects, little is known about the integration of glia into the host CNS. In this study, we have explored the potential of engrafted ESGPs to (1) undergo functional maturation, and (2) incorporate into the host glial network. To make these functional properties accessible to experimentation, we took advantage of an organotypic slice-culture paradigm that permits the study of donor cells under controlled conditions.

Materials and methods

Culture and labeling of ESGPs

Mouse ES cells (line J1) (Li et al., 1992) were aggregated to embryoid bodies and subsequently plated in ITSFn medium (Okabe et al., 1996). After 5 days, cells were trypsinized and propagated for 5 days in polyornithine-coated dishes in a DMEM/F12-based medium supplemented with 10 ng ml^{-1} FGF2. They were then harvested and replated in medium supplemented with FGF2 and EGF (20 ng ml^{-1}). In some experiments in vitro, the cells were propagated through an additional passage in medium supplemented with FGF2 and PDGF-AA (10 ng ml^{-1}, see Results). In vitro differentiation into astrocytes and oligodendrocytes was induced by growth-factor withdrawal as

described (Brüstle et al., 1999). Media, supplements and growth factors are available from Invitrogen (Karlsruhe, Germany), R&D (Wiesbaden, Germany) and Sigma (Taufkirchen, Germany). ESGPs proliferating in the presence of FGF2 and EGF were transfected with a CMV-GFP/neo expression construct (pEGFP-N1; Clontech, Palo Alto, CA) using FuGENE^{TM} 6 according to the manufacturers' instructions. For transplantation, cells selected in G418-containing medium were washed in Ca^{2+}/Mg^{2+}-free Hanks' buffered salt solution and concentrated to 80,000 cells μl^{-1}.

Slice culture and in vitro transplantation

Using a vibroslicer (VSLM1; Campden Instruments, Sileby, UK), 400-μm-thick slices encompassing the dentate gyrus, hippocampus and entorhinal/temporal cortex (Fig. 1A) were prepared from 9-day-old Wistar rats (Charles River, Sulzfeld, Germany). Slices were propagated as interface cultures (Stoppini et al., 1991) on clear polyester membranes (Transwell-Clear; Corning, Bodenheim, Germany). Media were changed on day one in culture and then on every other day. Although cultures were started in a horse-serum-containing medium, this was replaced gradually and at day 5 slices were cultured in a serum-free, defined solution based on DMEM/F12, and including N2 and B27 supplements (Cytogen, Sinn, Germany). The histoarchitecture of the majority of the slices (>75%) was remarkably well preserved for up to 5 weeks (Fig. 1B). Field excitatory postsynaptic potentials, recorded according to Newman et al., (Newman et al., 1995), revealed synaptic connectivity between perforant path and dentate gyrus as well as between Schaffer collaterals and CA1 pyramidal neurons for up to 33 days in culture (*n*=9; Fig. 1B inset). Anterograde tracing with rhodamine-conjugated dextran (Micro-Ruby®; Molecular Probes, Eugene, OR), performed as described by Kluge et al. (Kluge et al., 1998), confirmed the integrity of the perforant path (*n*=4; Fig. 1C) and TIMM staining showed an appropriate organization of the mossy fiber system (*n*=4; Fig. 1D) up to the end of the culture period.

In vitro transplantation was conducted at day 10±2 in culture. Using an injection device connected to a stereotactic frame (Stoelting, Wood Dale, IL), 1.0-2.5×10^4 ESGPs propagated in the presence of EGF and FGF and condensed to a total volume of 0.2 μl were deposited on the surface of the slice preparation in different locations [hilus of the dentate gyrus (DG), entorhinal cortex (EC) and temporal cortex (TC)]. Slices were washed thoroughly with medium to remove nonadherent donor cells 2 days after application. Fluorescence microscopy was used to monitor and document the distribution and morphology of the grafted cells at 2-day intervals. Proliferation of engrafted ESGPs was studied at days 2 and 10 after deposition. Slices were incubated with 10 μM BrdU (Sigma) for 48 hours, followed by thorough washing. BrdU-treated slices were excluded from functional studies and processed subsequently for immunofluorescence and confocal analysis (six slices at each time point).

Electrophysiology

Patch-clamp analysis of ESGPs on coverslips and in slice cultures was performed under continuous oxygenation in a bath solution containing (in mM): 150 NaCl, 5 KCl, 2 $MgSO_4$, 2 $CaCl_2$, 10 HEPES and 10 glucose, or DMEM/F12, pH 7.4 (with NaOH) as described (Kressin et al., 1995; Steinhäuser et al., 1994). The standard pipette solution contained (in mM): 130 KCl, 2 $MgCl_2$, 0.5 $CaCl_2$, 5 BAPTA, 10 HEPES, 3 Na_2ATP, and 0.1% Lucifer yellow (LY; Sigma), pH 7.25. Current signals were filtered at 3 or 10 kHz, and sampled at 5 or 30 kHz. Capacitance and series resistance compensation (up to 60%) were used to improve voltage-clamp control. Cells engrafted into slice cultures were identified by virtue of their green fluorescent protein (GFP) expression and chosen at random for functional analysis. During recording, donor cells were filled with LY by dialyzing the cytoplasm with the patch pipette solution. Following fixation, recorded cells were found at variable depths (20-110 μm) in the slice preparation. Double-immunolabeling with antibodies to glial fibrillary acidic protein (GFAP) and S100β was used to confirm the astroglial phenotype of the recorded cells (Fig. S1 and Table S1 at http://dev.biologists.org/supplmental).

Dye coupling

Slices were transferred to a submerged recording chamber (Luigs&Neumann; Neuss, Germany) and maintained under continuous oxygenation (95% O_2, 5% CO_2, 35°C). Using sharp microelectrodes (resistance 10-25 MΩ), 0.1% LY (Molecular Probes) was injected iontophoretically over a 30-minute period (Konietzko and Müller, 1994). Dye coupling was documented at 1 second, then at 1, 5, 7, 10, 15, 20, 25 and 30 minutes. Evaluation of dye spread was performed in fixed slices using confocal microscopy (Leica; Pulheim, Germany) and digital 3D reconstruction. Double immunolabeling with antibodies to M2 and GFAP or M2 and S100β confirmed the astroglial identity of both the injected donor cell and the coupled host-cell cluster.

Immunocytochemistry

For morphological analysis, the tissue was fixed in 4% paraformaldehyde, 15% picric acid and 0.1% glutaraldehyde (GA) for 15 minutes and postfixed without GA overnight at 4°C. Slices were then washed in PBS (Seromed; Berlin, Germany) and soaked in a phosphate-buffered 30% sucrose solution at 4°C overnight. Unless stated, series of 10 μm horizontal cryostat sections were prepared from each hippocampal slice specimen, mounted on either gelatin or polylysine-coated slides, air-dried and stored at 4°C until further use. ESGP invasion of host tissue was determined by evaluating the presence of GFP+ cell bodies in serial sections (*n*=27, see Results)

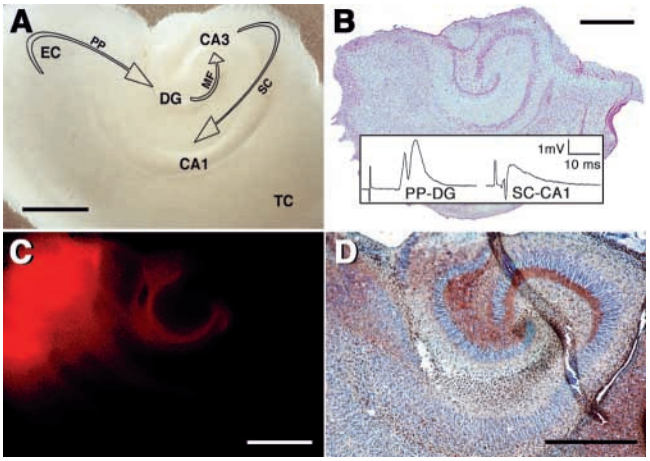

Fig. 1. Morphological and functional integrity of hippocampal slice cultures used as recipient tissue for ESGPs. (A) A 400 μm-thick slice one day after explantation. Dentate gyrus (DG), pyramidal-cell layer (CA3-CA1), entorhinal cortex (EC) and adjacent regions of the temporal cortex (TC) are well delineated. SC, Schaffer collaterals; MF, mossy fibers; PP, perforant path. (B) Cryostat section (10 μm) of a slice preparation maintained in culture for 31 days. Note the morphological preservation of the key anatomic structures (Hematoxylin and Eosin staining). The inset shows typical field potentials following orthodromic stimulation of the perforant path (PP-DG) and the Schaffer collaterals (SC-CA1) at the end of the culture period (stimulation artifacts blanked). (C) Anterograde tracing with rhodamine-conjugated dextran (Micro-Ruby®) confirms the integrity of the perforant path at 33 days in culture. (D) TIMM stain (performed according to Zimmer and Gähwiler, 1984) demonstrating the histological preservation of the MF system of a slice culture maintained for 33 days (20 μm cryostat section). Scale bars: 1 mm.

and in cross sections of fixed slice cultures (n=4) derived from three independent experiments. Data are expressed as mean±s.d. Statistical analysis was performed using the two-tailed Student's t-test. P values of <0.05 were considered significant.

For immunocytochemistry, a basic buffer was used that contained PBS (Seromed) and 10% fetal calf serum (Invitrogen). 0.1% Triton X-100 (Sigma) was added for the labeling of intracellular antigens. After preincubation in 5% normal goat serum (1-2 hours), primary antibodies to the following antigens were applied overnight at room temperature: BrdU (1:100, monoclonal; BD Biosciences, Heidelberg, Germany); CNP (1:100, monoclonal; Sigma); Connexin43 (1:300, polyclonal; Zymed, Berlin, Germany), GFAP (either 1:100, monoclonal; ICN, Costa Mesa, CA, or 1:400, polyclonal; DAKO, Hamburg, Germany); M2 (1:10, monoclonal; gift from C. Lagenaur); MBP (1:500, monoclonal; Chemicon, Temecula, CA); nestin (1:5, monoclonal; Rat-401, developed by Sue Hockfield and obtained from the Developmental Studies Hybridoma Bank, University of Iowa); NG2 (1:500, polyclonal; Chemicon); and S100β (1:5000, polyclonal; Swant, Bellinzona, Switzerland). After thorough washing, antigens were visualized by appropriate TRITC-, Cy3-, and Cy5-conjugated secondary antibodies (Vector, Burlingame, CA and Dianova, Hamburg, Germany) applied for 45 minutes at room temperature. Following another washing step, sections were mounted and analyzed using confocal microscopy and appropriate software for 3D reconstruction and image documentation (Leica). To determinate cell-type-specific antigen expression, 19 hippocampal slice cultures from days 11±4 after in vitro transplantation (from 4 independent experiments) were evaluated. For each antigen, immunofluorescence analysis of GFP+ cells was performed in 7-9 randomly assorted cryostat sections. Data are expressed as mean±s.d.

Results

Incorporation and differentiation of ESGPs in hippocampal slice cultures

Three stages of integration were observed following deposition of the donor cells on the slice surface (Fig. 2A): (1) vertical invasion into the slice; (2) horizontal migration within the host tissue; and (3) terminal differentiation in a variety of anatomical regions. Donor-cell invasion into the tissue was monitored at 1-2, 5-7, and 14-18 days after deposition (n=9 grafted slices at each time point) and seemed independent of the site of deposition. Incorporation at various depths of the slice preparation was assessed in serial sections and confirmed by cross sectioning the slice preparations (Fig. 2C). At 48 hours after deposition GFP+ cells had invaded the slice up to a depth of 90 μm (71.1±16.9 μm). Thereafter, migration activity decreased gradually. At 1 and 2 weeks after grafting, donor cells were found at up to 130 μm from the slice surface (90.0±20.0 μm and 96.7±15.8 μm, respectively). No significant difference in invasion depth was noted between days 5-7 and 14-18.

In addition to moving vertically into the host tissue, ESGPs spread horizontally inside the slice preparation. Donor cells migrated up to several hundred micrometers in the first week after engraftment (Fig. 2A,B). Migration inside the tissue occurred preferentially along endogenous fiber tracts. This was particularly prominent after deposition onto the EC (n=25), from where the transplanted cells distributed along the perforant path and the Schaffer collaterals. Cells placed onto the DG (n=16) spread throughout the DG hilar region, approaching the DG molecular layer and disseminating alongside the pyramidal cell layer. In contrast to EC and DG grafts, cells deposited onto the TC (n=13) spread less extensively and remained mostly confined to a halo around the engraftment site.

Independent of their location, the donor cells exhibited moderate mitotic activity during the first days after transplantation. Between days 2 and 4 post engraftment, 7.2±6.4% of the GFP+ cells incorporated BrdU (n=177). By

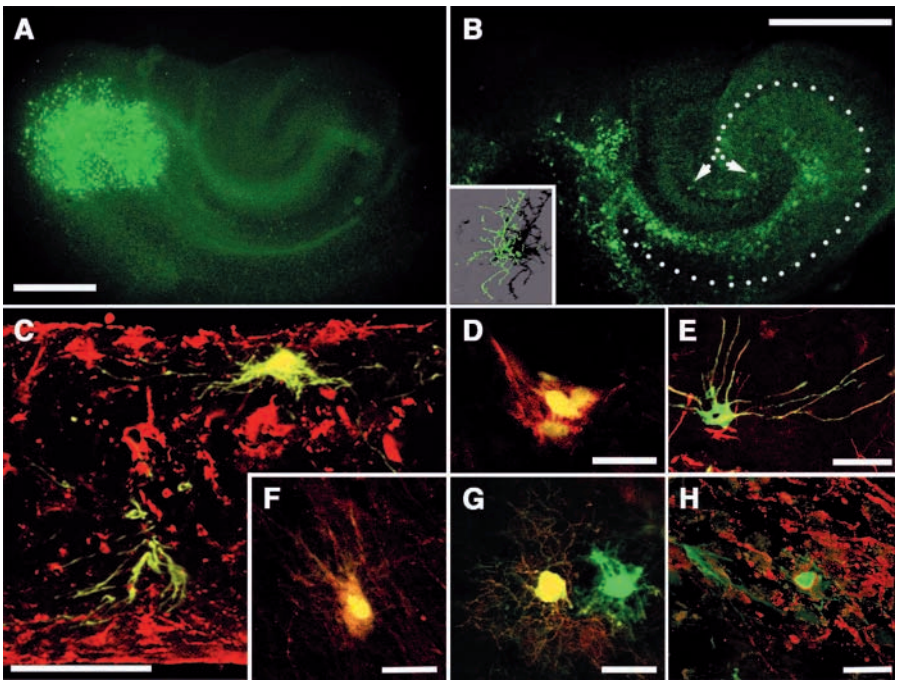

Fig. 2. In vitro transplantation of ESGPs in hippocampal slice cultures. (A) Slice culture one day after deposition of 20,000 GFP-labeled ESGPs onto the entorhinal cortex. (B) 18 days after implantation, the donor cells have migrated along the pyramidal cell layer and the Schaffer collaterals into the hilar region and the dentate granule cell layer (dashed line) where they developed complex 3D morphologies (inset, digital reconstruction of a grafted GFP-expressing cell composed of 32 individual planes). (C) At this same stage, cross sections through the entire slice preparation revealed donor cells incorporated at various depths in the host tissue. Double labeling with an antibody to GFAP (red). (D) Although some grafted cells retained an immature morphology and expressed NG2 (red), the majority exhibited differentiated glial phenotypes. (E) About 30% of the ESGPs were immunolabeled for nestin, including cells with astrocytic morphology. (F) In addition to GFAP, donor-derived astrocytes expressed S100β. (G) An ES cell-derived oligodendrocyte (in the EC region) identified using an antibody to CNP. (H) A GFP+ oligodendrocyte that expressed MBP (red) and had tubular processes that indicate myelin formation (stratum oriens, CA1). Scale bars: in A,B, 1 mm; in C, 100 μm; in D-H, 25 μm.

contrast, no BrdU uptake was observed in 144 GFP+ cells evaluated between days 10 and 12 after engraftment. Thus, donor-cell migration and proliferation ceased in the second week after transplantation.

During the first week after deposition, most GFP+ cells had bipolar, migratory phenotypes. In the second week, they developed increasingly multipolar, astrocytic and oligodendroglial morphologies. Immunofluorescence analyses at 11±4 days after deposition revealed that 9.4±5.6% (*n*=212) of GFP-labeled cells expressed NG2, a marker of glial precursors (Fig. 2D) (Diers-Fenger et al., 2001). Nestin immunoreactivity was retained in 30.4±9.3% of the cells (*n*=280). Astrocytes expressed GFAP (27.5±6.2%, *n*=251) and/or S100β (40.5±7.7%, *n*=227) and had a nonpolarized morphology with round-oval cell bodies from which emanated numerous prominent processes (Fig. 2F). Many process-bearing cells with astrocytic morphology expressed nestin (Fig. 2E). Typically, donor-derived CNP+ oligodendrocytes (30.3±9.8%, *n*=238) had small, round cell bodies with delicate branched processes (Fig. 2G). No correlation was noted between donor-cell differentiation and association with specific anatomical compartments. However, some GFP+ oligodendrocytes bearing characteristic tubular processes were found either in clusters or individually within fiber bundles of the recipient tissue (e.g. in the CA3-CA1 molecular layer, the alveus and the subgranular layer of the DG). The longer the time after deposition, the more these cells expressed myelin basic protein (MBP; Fig. 2H). Whereas the 'tubular' appearance of the cell processes and the expression of CNP and MBP indicated that some of the donor cells had differentiated into myelinating oligodendrocytes, ultrastructural studies are required to confirm this assumption.

In summary, the morphological and immunohistochemical data indicate that most ESGPs undergo terminal differentiation into astroglia and oligodendroglia by two weeks after implantation.

Changing functional properties of engrafted ESGPs

Patch-clamp analysis was used to study the functional characteristics of ESGPs incorporated into the hippocampus and to compare them with ESGPs that proliferate and differentiate in monolayer cultures in the absence of host tissue. Whole-cell currents were elicited by stepping the membrane to increasing depolarizing and hyperpolarizing potentials between –160 and +20 mV (50 ms, holding potential –70 mV, see Fig. 3A,B insets). Delayed rectifier outward K^+ currents [$I_{K(D)}$] were isolated by depolarizing the membrane to –40 mV for 300 ms. This pre-pulse was followed by a 3 ms interval at –70 mV, and then the membrane was stepped up to +70 mV (Fig. 3C, middle). Transient outward K^+ currents [$I_{K(A)}$] were separated by subtracting the outward currents evoked after the –40 mV pre-pulses from those activated after a –110 mV pre-pulse (Fig. 3C, right). In the presence of FGF2 and EGF, ESGPs proliferated (Brüstle et al., 1999) and displayed the properties of immature glia, with all cells (*n*=9) expressing $I_{K(D)}$ (Fig. 3A). $I_{K(A)}$ was present in 3/9 cells. Inwardly rectifying K^+ (I_{Kir}) and background K^+ currents [$I_{K(P)}$], which are characteristic of mature glia (Bordey et al., 2001; Verkhratsky and Steinhäuser, 2000), could not be demonstrated.

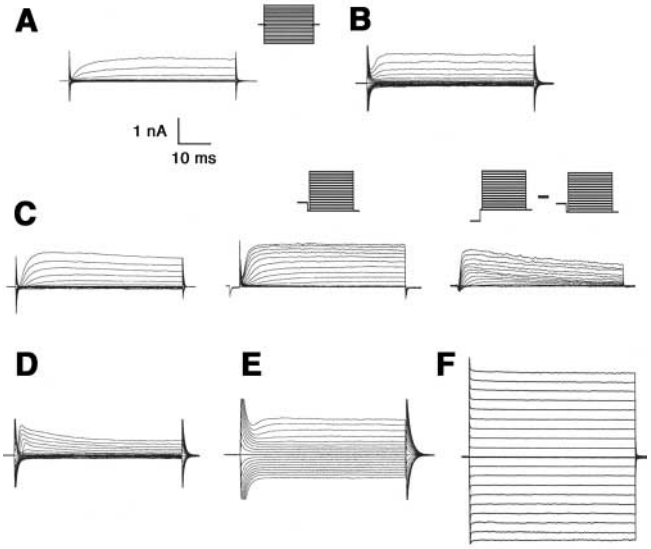

Fig. 3. Patch clamp analysis of ESGPs before and after transplantation. (A-C) Cultured ESGPs exhibit $I_{K(A)}$ and/or $I_{K(D)}$ but lack I_{Kir} and $I_{K(P)}$. The current pattern during propagation in EGF/FGF (A), PDGF/FGF (B), and 9 days after growth factor withdrawal (C) are shown. (D-F) After transplantation, ESGPs have three distinct current patterns. Whereas some cells retain the immature pattern observed during monolayer culture (D), others display I_{Kir} (E). The majority of engrafted ESGPs displayed prominent $I_{K(P)}$ (F). Current phenotypes shown in E,F are characteristic of mature hippocampal astrocytes in vivo. The pulse protocol (see text) used in A,B also applies to (C, left) and (D-F).

Table 1. Functional parameters of ESGPs growing in monolayer culture and following incorporation into hippocampal slice cultures

	Monolayer culture				6-15 days after in vitro transplantation		
	EGF/FGF	PDGF/FGF	3 DGW	9 DGW	Without I_{Kir}	With I_{Kir}	With $I_{K(P)}$
V_r [mV]	–27.1±5.2 (9)	–31.3±9.3 (11)	–28.3±6.8 (17)	–48.6±14.5 (8)	–27±5.1 (3)	–43.5±14 (4)	–62.7±2.1 (11)
C_M [pF]	7.8±6.5 (9)	7.9±6.2 (11)	5.8±4.9 (17)	7.4±2.8 (8)	7.5±2.1 (4)	n.d.	n.d.
$I_{K(A),\ +70mV}$ [pA/pF]	61.1±35.2 (3)	164±84.5 (9)	158±74.8 (15)	153±123 (8)	159±98 (3)	382±144 pA (3)	–
$I_{K(D),\ +70\ mV}$ [pA/pF]	200±106 (9)	235±150 (10)	158±53.1 (17)	167±51.9 (8)	149±58 (3)	1.7±0.5 nA (7)	–
$I_{Kir,\ -130\ mV}$ [pA]	–	–	–	–	–	605±318 (7) (7)	–
$I_{K(P),\ +70\ mV}$ [nA]	–	–	–	–	–	–	2.2±1.5 (20)

In monolayer culture, ESGPs were propagated in the presence of EGF/FGF and, subsequently, PDGF/FGF. In vitro differentiation was induced by subsequent withdrawal from PDGF/FGF for 3 or 9 days. Note that cells expressing I_{Kir} or $I_{K(P)}$ were not observed under either monolayer condition (see Results). DGW, days after withdrawal from PDGF/FGF. C_M not determined (n.d.) owing to putative gap junction coupling. Cell numbers are in parentheses.

Culture conditions that promote differentiation of ESGPs in vitro (Brüstle et al., 1999), such as propagation in FGF2 and PDGF (Fig. 3B; *n*=11) and subsequent growth factor withdrawal (Fig. 3C; *n*=25), did not alter significantly the mean resting potential, membrane capacitance and current densities. I_{Kir} and $I_{K(P)}$ remained undetectable even 9 days after growth factor withdrawal in vitro (Table 1).

By contrast, functional properties that are characteristic of mature glia were observed in the majority of ESGPs following integration into hippocampal slice cultures. Based on their current patterns, three subpopulations of donor-derived astrocytes could be distinguished on days 6-20 after engraftment (Table 1, Fig. 3D-F; see also Fig. S1 and Table S1 at http://dev.biologists.org/supplmental). A small proportion of GFP+ cells (4/31) expressed voltage-activated currents but lacked I_{Kir} and $I_{K(P)}$, which resembled ESGPs before transplantation (Fig. 3D). A second group (7/31) exhibited I_{Kir} in addition to voltage-activated currents (Fig. 3E). A third population (20/31, >60%) of the recorded donor-derived astrocytes had prominent $I_{K(P)}$ typically found in 'passive' glial cells in mature hippocampus (Fig. 3F) (Kressin et al., 1995; Steinhäuser et al., 1992). There was no obvious association between these functional phenotypes and specific anatomical structures.

Tail current analysis of I_{Kir} and $I_{K(P)}$ revealed reversal potentials of –61.3±13 mV (*n*=3) and –68.4±8.9 mV (*n*=9), which indicates that these currents were mainly carried by K^+ ions (data not shown). Similar to astrocyte development in vivo, the resting potential of the grafted cells decreased in response to an increasing contribution of I_{Kir} and $I_{K(P)}$ (Table 1).

ES cell-derived astrocytes establish gap junctions with recipient glia

A hallmark of astrocyte development in vivo is the formation of gap junctions. Individual astrocytes are coupled to dozens of neighboring cells to form an extensive syncytial network of interconnected glia (Giaume and McCarthy, 1996). We were interested in whether transplanted ES cell-derived astrocytes are inserted into such a network structure. To assess gap junction coupling, incorporated GFP+ astrocytes were filled with LY (Fig. 4, Fig. 5A). Cells were chosen randomly, taking care that no other GFP+ donor cells were present in the vicinity of the injected cell. Typically, LY spread from the incorporated ES cell-derived astrocyte to one or two neighboring host glia cells (Fig. 4A). From there, dye diffusion proceeded in all three dimensions, decorating additional astrocytes of the host glial network. The resulting LY-filled cell clusters were reminiscent of the astroglial syncytium in native rodent hippocampus (Konietzko and Müller, 1994; Theis et al., 2003). After fixation, dye coupling was quantified using digital 3D-reconstructions of LY-filled cell clusters (Fig. 4B). Three weeks after deposition, individual donor cells filled with LY for 30 minutes were coupled with up to 50 endogenous astrocytes (34±8). Subsequent serial sectioning of the hippocampal tissue and immunofluorescence analysis using the mouse-specific antibody M2 (Lagenaur and Schachner, 1981) confirmed the presence of a single, donor-derived astrocyte in each cluster of LY-filled cells (Fig. 4C,D). The remainder of cells represented endogenous astrocytes that expressed S100β and/or GFAP. No LY-filled neurons were observed in the coupled cell clusters (data not shown).

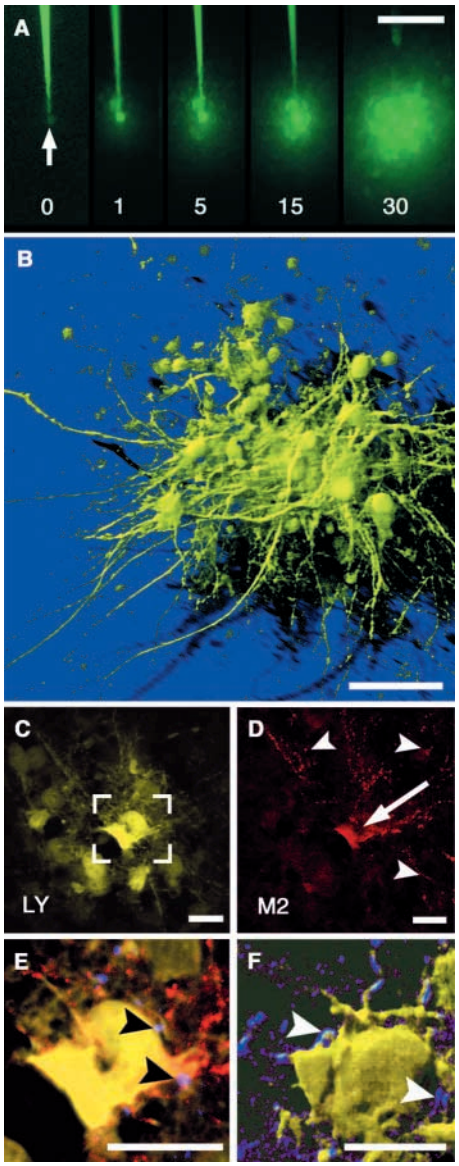

Fig. 4. Glial network integration of ES cell-derived astrocytes. (A) Epifluorescence microscopy during a 30-minute iontophoretic injection of LY into a GFP-labeled donor cell, located at the border of EC and subiculum (arrow, 25 days after transplantation; both LY and GFP signals are recorded in the FITC channel). Note the extensive dye coupling to adjacent host cells. (B) Confocoal microscopy and 3D reconstruction of (A), reveals a cluster of 50 coupled cells with total volume of 5.6×10^{-3} mm^3. The picture is taken following fixation and depicts the 3D nature of the endogenous glial network. (C-D) Subsequent serial sectioning and double labeling with an antibody to the mouse-specific antigen M2 (red) confirms the donor origin of the injected astrocyte depicted in A. Note the extensive arborization (arrowheads) and the perforation of the cell body (arrow). (E) Overlay of C and D (boxed area delineated in C), triple labeled with an antibody to connexin43 (blue). Patches of connexin43 immunoreactivity (arrowheads) are detected at the contact zones between the LY/M2+ donor cell and two adjacent LY-filled host-cell processes. (F) Prominent connexin43 expression (blue) is also observed on LY-filled processes connecting individual host cells of the same cluster (confocal 3D reconstruction). Note that figures A-F are from the same donor-host cell cluster. Scale bars: in A, 200 μm; in B, 50 μm; in C-F, 25 μm.

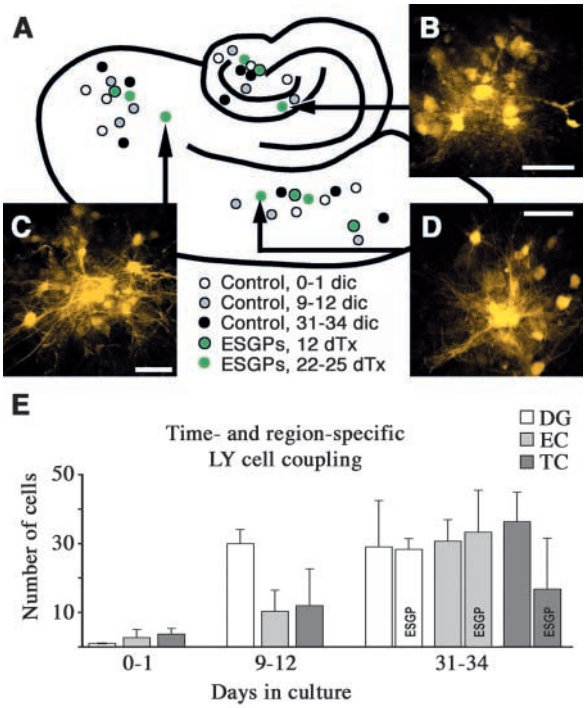

Fig. 5. Regional distribution and time course of cell-cell coupling. (A) Schematic representation of endogenous and incorporated ESGP-derived astrocytes used for analysis of network integration. (B-D) Examples of host-cell clusters coupled to individual GFP+ donor cells as seen by confocal analysis (each shown as overlay of 32 individual scans). After engraftment for 22-25 days, donor-derived astrocytes integrated equally well in glial networks of different anatomical regions of the recipient slice [molecular layer of the DG in B, EC/subiculum in C (as in Fig. 4B), TC region in D]. Both LY and GFP signals are recorded in the FITC channel. (E) Cell coupling of endogenous and engrafted ESGPs in three hippocampal subregions at different times in culture. Endogenous astrocytes reveal an increasing complexity of gap junction coupling during the culture period. After transplantation for 2-3 weeks, coupling ratios between donor and host cells in DG and EC equal those observed between endogenous astrocytes (engrafted slices were analyzed 12-25 days after donor cell deposition described in A). DG, dentate gyrus; dic, days in culture; dTx, days after deposition; EC, entorhinal cortex; TC, temporal cortex. Scale bars: 50 μm.

Connexin43 (Cx43) has been identified as a key component of astrocyte-astrocyte gap junctions (Rash et al., 2001; Theis et al., 2003). Double labeling of M2+ and LY-filled cells with an antibody to Cx43 demonstrated patches of immunoreactivity at contact zones between donor and host processes as well as between adjacent LY-labeled host cells (Fig. 4E,F).

Dye coupling of donor cells appeared to be independent of their location in the slice preparation. All donor cells (n=6) studied at 22-25 days after engraftment revealed extensive dye coupling to adjacent host glia (Fig. 5A-D). Out of four donor cells injected 12 days after engraftment, only three exhibited dye coupling (Fig. 5A,E). The spread of LY from these cells was limited to three (TC region), 21 (EC region), and 24 (DG region) host cells, respectively. In addition, one donor cell in the TC region did not appear to be connected to the endogenous glial network. Although more detailed analyses are required to interpret these observations, they could indicate regional differences in the efficiency of glial gap junction formation. However, the differences observed might simply reflect the dynamic nature of gap junction coupling in astrocytes (Giaume and McCarthy, 1996).

We next studied the time course of endogenous glial cell coupling and whether coupling between host cells is affected by incorporated ESGPs. Dye coupling was performed at days 0-2, 9-12 and 31-34 in culture, using hippocampal slices not subjected to in vitro transplantation (nine cells in nine individual slices at each time point; Fig. 5A). In accordance with in vivo studies in rodent CNS (Binmöller and Müller, 1992; Kressin et al., 1995), the complexity of gap junction coupling between host astrocytes increased with time in culture and maturation of the tissue (Fig. 5E). Implanting ESGPs appeared to have no effect on the development of gap junctions between host cells. No morphological differences were observed between LY-labeled donor-host and host-host cell clusters, and junctional coupling between donor and host cells also increased with time in culture.

In all, nine out of 10 injected donor-derived astrocytes were coupled with host cells, demonstrating that integration of grafted ESGPs into the glial network is a robust phenomenon. The increase in coupling efficiency with the time in culture indicates that the recruitment of ES cell-derived glial precursors into the endogenous glial network depends on the developmental stage of the host tissue.

Discussion

The results of this study have important implications for both the methodology of studying stem cell integration into CNS tissue and the potential use of ES cell-derived glia in neural repair. From a methodological perspective, we have shown that hippocampal slice cultures represent a versatile model system to study the morphological and functional properties of neural donor cells engrafted into host CNS tissue. Applying this technique to ES cell-derived precursors, we provide evidence for the functional maturation of glial precursors following incorporation into the hippocampus. Our data demonstrate that the electrophysiological properties of incorporated ES cell-derived glial cells resemble those of native glia. Last, we show that ESGP-derived astrocytes establish gap junctions with recipient glia and become part of the endogenous glial network. This latter finding could provide an interesting approach for the widespread, direct delivery of recombinant factors from genetically modified donor cells.

An in vitro model for neural transplantation

Organotypic hippocampal slice cultures represent a 3D model system of the CNS that is used increasingly to study a variety of developmental and disease-related processes (Gähwiler et al., 1997; McKinney et al., 1997; Ullrich et al., 2001). In the past, the introduction of donor cells into CNS slice cultures has been employed successfully for the analysis of donor cell attachment (Förster et al., 1998), neurite outgrowth (Shetty and Turner, 1999), and microglia and glioma cell invasion (Hailer et al., 1997; Ohnishi et al., 1998).

Refining the methodology, we have established conditions that permit the propagation of vital, functionally active hippocampal slice preparations for up to 5 weeks in serum-free

media. We observed a remarkable preservation of the neuronal subpopulations (Fig. 1B,D) and functional maintenance of the fiber tracts (Fig. 1B inset; Fig. 1C,D). Used as 'recipient' tissue, this culture system provides an opportunity to study the incorporation, differentiation and function of neural precursors in unprecedented detail. ESGPs deposited on the surface of the slice rapidly invaded the preparation and continued to migrate within the tissue (Fig. 2A,B). After a 2-week period, migration ceased and postmitotic donor cells with complex 3D morphologies were found at various depths of the slice preparation (Fig. 2B inset). Immunohistochemical analyses revealed that the incorporated bipotential ESGPs differentiate into astroglial and oligodendroglial phenotypes (Fig. 2C-G). Thus, this model system provides optimal prerequisites for a functional analysis of engrafted precursor cells.

Engrafted ES cell-derived glial cells undergo functional maturation

Unlimited self-renewal, pluripotency and amenability to genetic manipulation make ES cells a highly attractive donor source for cell replacement. We have shown previously that bipotential glial precursors can be efficiently derived from mouse ES cells. These cells proliferate in the presence of FGF2 and EGF and, upon growth factor withdrawal, differentiate into astrocytes and oligodendrocytes. Although ES cell-derived oligodendrocytes repair myelin in dysmyelinating mutants (Brüstle et al., 1999), the functional properties of integrated ESGPs remain unclear.

During normal development, differentiating astrocytes undergo a characteristic change of ion channel expression (Kressin et al., 1995). Whereas predominating voltage-activated K^+ currents are characteristic of immature astrocytes, I_{Kir} and $I_{K(P)}$ are expressed in more mature glia (Bordey et al., 2001; Verkhratsky and Steinhäuser, 2000). We found that ESGPs proliferating in monolayer cultures express only voltage-gated K^+ currents (Fig. 3A). Interestingly, differentiation induced by growth factor withdrawal did not elicit I_{Kir} and $I_{K(P)}$ (Fig. 3B,C). It was only after incorporation into hippocampal slice cultures that most GFP-labeled donor-derived astrocytes expressed prominent I_{Kir} or $I_{K(P)}$ (Fig. 3E,F). These data provide the first evidence for functional maturation of transplanted glial precursors. Moreover, they indicate that these cells might adopt the distinct astroglial phenotypes that exist in vivo (Matthias et al., 2003). The dynamic changes in ion currents observed following engraftment of ESGPs into hippocampal slice cultures appear to recapitulate developmental patterns in vivo. The absence of I_{Kir} and $I_{K(P)}$ during propagation in vitro indicates that full, functional maturation of ESGPs depends on additional environmental cues in the recipient brain tissue.

It is difficult to address whether the electrophysiological properties of the engrafted donor-derived astrocytes represent a normal or a 'reactive' state. Functional data from acute brain slices indicate that, in lesioned or sclerotic CNS, there is a dramatic reduction in the number of astrocytes with a 'passive' current phenotype and a downregulation of astrocytic I_{Kir} in the remaining astrocytes (Bordey et al., 2001; Hinterkeuser et al., 2000; Schröder et al., 1999). Certainly, the organotypic cell culture imposes environmental conditions on the cells distinct from in vivo conditions. Hence, quantitative comparison of biophysical parameters (e.g. I_{Kir} density) between cells in culture and in situ does not seem sensible. However, the qualitative changes we observed during development after engraftment (i.e. upregulation of I_{Kir} density and the appearance of astrocytes with a passive current phenotype) resemble aspects of astroglial maturation in vivo, and are opposite to the alterations that astrocytes undergo in response to brain damage and disease. Thus, we conclude that donor cells expressing significant I_{Kir} densities or a dominant passive current phenotype represent 'normal' astrocytes whereas ES cell-derived astrocytes that lack I_{Kir} might represent a 'reactive' state.

Glial network integration of grafted ES cell-derived astrocytes

Gap junction coupling between hippocampal astrocytes is established gradually during early postnatal development (Binmöller and Müller, 1992; Konietzko and Müller, 1994). This phenomenon is preserved in hippocampal slice cultures where endogenous astrocytes show an increased amount of dye coupling with time in culture (Fig. 5E). Surprisingly, ESGPs introduced into different areas of hippocampal tissue possess a remarkable capacity to integrate into this network structure (Fig. 5A-D). Functional dye coupling between donor and host cells was verified by injecting LY, a low-molecular-weight fluorescent dye, into individual donor-derived astrocytes (Fig. 4A,B). Following injection of an individual donor cell, LY spread typically into one or two neighboring host cells before distributing further into the adjacent glia. This indicates that coupling to one or two host cells is sufficient to efficiently integrate the donor cells into the established host glial network. This is supported by the observation that coupling ratios between donor and host cells were comparable to those observed among the endogenous cells (Fig. 5E).

Gap junctions are composed of connexin molecules that form pores between neighboring astrocytes (Giaume and McCarthy, 1996). Permeable to ions and small signaling molecules, gap junctions are thought to play an important role in spatial ion buffering and functional synchronization of the glial network. Connexin43, the key component of astrocyte-astrocyte gap junctions (Rash et al., 2001; Theis et al., 2003), was detected consistently at contact zones between incorporated donor cells and adjacent processes of host cells (Fig. 4C-F).

We found no evidence of gap junction coupling between engrafted ES cell-derived astrocytes and host neurons, such as described between endogenous cells in some CNS regions (Alvarez-Maubecin et al., 2000; Rash et al., 2001). However, mechanisms of glio-neuronal interactions become increasingly well defined (e.g. Aguado et al., 2002; Haydon, 2001; Kojima et al., 1999; Verkhratsky and Steinhäuser, 2000), and it is tempting to speculate that the transplanted cells might communicate with neurons via pathways other than junctional coupling. Considering that ESGPs appear to integrate into any given glial network structure and that neuronal cells can be easily included in the grafted population, the slice culture paradigm might be particularly useful for addressing these issues.

Currently, it is unclear whether and to what extent the integrated ES cell-derived astrocytes elicit functional changes in endogenous glial cells and whether they affect functioning

of host neurons. However, on a translational level, gap junction coupling between donor and host glia might offer previously unrecognized opportunities for transplant-based treatment strategies. The introduction of genetically modified astrocytes into the host network could permit transcellular delivery of small foreign molecules to large areas of the CNS. Considering the amenability of ES cells to genetic modification, such a strategy might be used for compound delivery as well as for transglial modification of neuronal function.

Potential and caveats of the slice culture paradigm

Used as an 'in vitro transplantation' model, the slice culture system offers a number of advantages. In contrast to in vivo grafts, it permits direct experimental access to donor cell migration and integration. Direct visualization allows precise placement of very small cell numbers. The ex vivo approach circumvents immunological problems and facilitates the analysis of allogeneic or xenogeneic donor cells. Last, the model can accommodate donor cells and host tissues from different genetic backgrounds, which enables a broad range of transgenic studies.

Devised as a reductionist model, the 'graft-in-a-slice' paradigm also has several limitations. Deposition of the donor cells on the slice surface restricts the analysis to the cells that invade the slice tissue within 48 hours. Thus, more differentiated cells with reduced migratory potential might escape analysis. In addition, differences are expected with respect to the efficiency with which individual donor cell types can be studied in different slice tissues. Although we have focused primarily on the properties of ES cell-derived astrocytes, the morphological data and the expression of myelin proteins by incorporated donor cells indicate that the slice culture paradigm could, in principle, be well suited for studying oligodendrocyte-axon interactions as well as functional implications of donor-derived myelin formation. However, because the postnatal hippocampus contains only few myelinated areas (although preserved in the interphase culture conditions applied here) (Berger and Frotscher, 1994), slice cultures from other brain regions such as the cerebellum might be more suitable for addressing topics associated with myelin formation (Dusart et al., 1997; Seil, 1989).

Despite the organotypic and functional preservation of the slice tissue, great care should be taken when extrapolating results to in vivo conditions. Factors produced by reactive or proliferative astroglia and microglia as well as reorganizing neuronal subpopulations are known to complicate the interpretation of slice culture data (Caesar and Aertsen, 1991; del Rio et al., 1991; Derouiche et al., 1993; Hailer et al., 1996). Thus, although it improves accessibility and provides a highly controlled experimental setting, the slice culture system is suited primarily to providing proof-of-principle data that can be validated in an in vivo scenario.

This work was supported by the Hertie Foundation, the BONFOR program, the Innovationsprogramm Forschung des Landes Nordrhein-Westfalen, the Bundesministerium für Bildung und Forschung (01GN0108) and the Deutsche Forschungsgemeinschaft (SFB TR3). We would like to thank Ilker Eyüpoglu for his help in setting up the slice culture system, Stefan Hinterkeuser for supporting the patch clamp studies and Holger Rothkegel for performing the TIMM stainings.

References

Aguado, F., Espinosa-Parrilla, J. F., Carmona, M. A. and Soriano, E. (2002). Neuronal activity regulates correlated network properties of spontaneous calcium transients in astrocytes in situ. *J. Neurosci.* **22**, 9430-9444.

Alvarez-Maubecin, V., Garcia-Hernandez, F., Williams, J. T. and Van Bockstaele, E. J. (2000). Functional coupling between neurons and glia. *J. Neurosci.* **20**, 4091-4098.

Berger, T. and Frotscher, M. (1994). Distribution and morphological characteristics of oligodendrocytes in the rat hippocampus in situ and in vitro: an immunocytochemical study with the monoclonal Rip antibody. *J. Neurocytol.* **23**, 61-74.

Binmöller, F. J. and Müller, C. M. (1992). Postnatal development of dye-coupling among astrocytes in rat visual cortex. *Glia* **6**, 127-137.

Bordey, A., Lyons, S. A., Hablitz, J. J. and Sontheimer, H. (2001). Electrophysiological characteristics of reactive astrocytes in experimental cortical dysplasia. *J. Neurophysiol.* **85**, 1719-1731.

Brüstle, O., Jones, K. N., Learish, R. D., Karram, K., Choudhary, K., Wiestler, O. D., Duncan, I. D. and McKay, R. D. (1999). Embryonic stem cell-derived glial precursors: a source of myelinating transplants. *Science* **285**, 754-756.

Caeser, M. and Aertsen, A. (1991). Morphological organization of rat hippocampal slice cultures. *J. Comp. Neurol.* **307**, 87-106.

del Rio, J. A., Heimrich, B., Soriano, E., Schwegler, H. and Frotscher, M. (1991). Proliferation and differentiation of glial fibrillary acidic protein-immunoreactive glial cells in organotypic slice cultures of rat hippocampus. *Neuroscience* **43**, 335-347.

Derouiche, A., Heimrich, B. and Frotscher, M. (1993). Loss of layer-specific astrocytic glutamine synthetase immunoreactivity in slice cultures of hippocampus. *Eur. J. Neurosci.* **5**, 122-127.

Diers-Fenger, M., Kirchhoff, F., Kettenmann, H., Levine, J. M. and Trotter, J. (2001). AN2/NG2 protein-expressing glial progenitor cells in the murine CNS: isolation, differentiation, and association with radial glia. *Glia* **34**, 213-228.

Dusart, I., Airaksinen, M. S. and Sotelo, C. (1997). Purkinje cell survival and axonal regeneration are age dependent: an in vitro study. *J. Neurosci.* **17**, 3710-3726.

Förster, E., Kaltschmidt, C., Deng, J., Cremer, H., Deller, T. and Frotscher, M. (1998). Lamina-specific cell adhesion on living slices of hippocampus. *Development* **125**, 3399-3410.

Gähwiler, B. H., Capogna, M., Debanne, D., McKinney, R. A. and Thompson, S. M. (1997). Organotypic slice cultures: a technique has come of age. *Trends Neurosci.* **20**, 471-477.

Gates, M. A., Olsson, M., Bjerregaard, K. and Bjorklund, A. (1998). Region-specific migration of embryonic glia grafted to the neonatal brain. *Neuroscience* **84**, 1013-1023.

Giaume, C. and McCarthy, K. D. (1996). Control of gap-junctional communication in astrocytic networks. *Trends Neurosci.* **19**, 319-325.

Hailer, N. P., Heppner, F. L., Haas, D. and Nitsch, R. (1997). Fluorescent dye prelabelled microglial cells migrate into organotypic hippocampal slice cultures and ramify. *Eur. J. Neurosci.* **9**, 863-866.

Hailer, N. P., Jarhult, J. D. and Nitsch, R. (1996). Resting microglial cells in vitro: analysis of morphology and adhesion molecule expression in organotypic hippocampal slice cultures. *Glia* **18**, 319-331.

Haydon, P. G. (2001). GLIA: listening and talking to the synapse. *Nat. Rev. Neurosci.* **2**, 185-193.

Hinterkeuser, S., Schröder, W., Hager, G., Seifert, G., Blümcke, I., Elger, C. E., Schramm, J. and Steinhäuser, C. (2000). Astrocytes in the hippocampus of patients with temporal lobe epilepsy display changes in potassium conductances. *Eur. J. Neurosci.* **12**, 2087-2096.

Kluge, A., Hailer, N. P., Horvath, T. L., Bechmann, I. and Nitsch, R. (1998). Tracing of the entorhinal-hippocampal pathway in vitro. *Hippocampus* **8**, 57-68.

Kojima, S., Nakamura, T., Nidaira, T., Nakamura, K., Ooashi, N., Ito, E., Watase, K., Tanaka, K., Wada, K., Kudo, Y. et al. (1999). Optical detection of synaptically induced glutamate transport in hippocampal slices. *J. Neurosci.* **19**, 2580-2588.

Konietzko, U. and Müller, C. M. (1994). Astrocytic dye coupling in rat hippocampus: topography, developmental onset, and modulation by protein kinase C. *Hippocampus* **4**, 297-306.

Kressin, K., Kuprijanova, E., Jabs, R., Seifert, G. and Steinhäuser, C. (1995). Developmental regulation of Na+ and K+ conductances in glial cells of mouse hippocampal brain slices. *Glia* **15**, 173-187.

Lagenaur, C. and Schachner, M. (1981). Monoclonal antibody (M2) to glial

and neuronal cell surfaces. *J. Supramol. Struct. Cell. Biochem.* **15**, 335-346.

Li, E., Bestor, T. H. and Jaenisch, R. (1992). Targeted mutation of the DNA methyltransferase gene results in embryonic lethality. *Cell* **69**, 915-926.

Matthias, K., Kirchhoff, F., Seifert, G., Hüttmann, K., Matyash, M., Kettenmann, H. and Steinhäuser, C. (2003). Segregated expression of AMPA-type glutamate receptors and glutamate transporters defines distinct astrocyte populations in the mouse hippocampus. *J. Neurosci.* **23**, 1750-1758.

McKinney, R. A., Debanne, D., Gähwiler, B. H. and Thompson, S. M. (1997). Lesion-induced axonal sprouting and hyperexcitability in the hippocampus in vitro: implications for the genesis of posttraumatic epilepsy. *Nat. Med.* **3**, 990-996.

Newman, G. C., Hospod, F. E., Qi, H. and Patel, H. (1995). Effects of dextran on hippocampal brain slice water, extracellular space, calcium kinetics and histology. *J. Neurosci. Methods* **61**, 33-46.

Ohnishi, T., Matsumura, H., Izumoto, S., Hiraga, S. and Hayakawa, T. (1998). A novel model of glioma cell invasion using organotypic brain slice culture. *Cancer Res.* **58**, 2935-2940.

Okabe, S., Forsberg-Nilsson, K., Spiro, A. C., Segal, M. and McKay, R. D. (1996). Development of neuronal precursor cells and functional postmitotic neurons from embryonic stem cells in vitro. *Mech. Dev.* **59**, 89-102.

Rash, J. E., Yasumura, T., Dudek, F. E. and Nagy, J. I. (2001). Cell-specific expression of connexins and evidence of restricted gap junctional coupling between glial cells and between neurons. *J. Neurosci.* **21**, 1983-2000.

Schröder, W., Hager, G., Kouprijanova, E., Weber, M., Schmitt, A. B., Seifert, G. and Steinhäuser, C. (1999). Lesion-induced changes of electrophysiological properties in astrocytes of the rat dentate gyrus. *Glia* **28**, 166-174.

Seil, F. J. (1989). Tissue culture models of myelination after oligodendrocyte transplantation. *J. Neural Transplant* **1**, 49-55.

Shetty, A. K. and Turner, D. A. (1999). Neurite outgrowth from progeny of epidermal growth factor-responsive hippocampal stem cells is significantly less robust than from fetal hippocampal cells following grafting onto organotypic hippocampal slice cultures: effect of brain-derived neurotrophic factor. *J. Neurobiol.* **38**, 391-413.

Song, H. J., Stevens, C. F. and Gage, F. H. (2002). Astroglia induce neurogenesis from adult neural stem cells. *Nature* **417**, 39-44.

Steinhäuser, C., Berger, T., Frotscher, M. and Kettenmann, H. (1992). Heterogeneity in the membrane current pattern of identified glial cells in the hippocampal slice. *Eur. J. Neurosci.* **4**, 472-484.

Steinhäuser, C., Kressin, K., Kuprijanova, E., Weber, M. and Seifert, G. (1994). Properties of voltage-activated Na+ and K+ currents in mouse hippocampal glial cells in situ and after acute isolation from tissue slices. *Pflugers Arch.* **428**, 610-620.

Stoppini, L., Buchs, P. A. and Müller, D. (1991). A simple method for organotypic cultures of nervous tissue. *J. Neurosci. Methods* **37**, 173-182.

Svendsen, C. N. and Smith, A. G. (1999). New prospects for human stem-cell therapy in the nervous system. *Trends Neurosci.* **22**, 357-364.

Theis, M., Jauch, R., Zhuo, L., Speidel, D., Wallraff, A., Doring, B., Frisch, C., Sohl, G., Teubner, B., Euwens, C. et al. (2003). Accelerated hippocampal spreading depression and enhanced locomotory activity in mice with astrocyte-directed inactivation of connexin43. *J. Neurosci.* **23**, 766-776.

Ullrich, O., Diestel, A., Eyüpoglu, I. Y. and Nitsch, R. (2001). Regulation of microglial expression of integrins by poly(ADP-ribose) polymerase-1. *Nat. Cell Biol.* **3**, 1035-1042.

Verkhratsky, A. and Steinhäuser, C. (2000). Ion channels in glial cells. *Brain Res. Brain Res. Rev.* **32**, 380-412.

Zhou, H. and Lund, R. D. (1993). Effects of the age of donor or host tissue on astrocyte migration from intracerebral xenografts of corpus callosum. *Exp. Neurol.* **122**, 155-164.

Zimmer, A. (1992). Manipulating the genome by homologous recombination in embryonic stem cells. *Annu. Rev. Neurosci.* **15**, 115-137.

Zimmer, J. and Gähwiler, B. H. (1984). Cellular and connective organization of slice cultures of the rat hippocampus and fascia dentata. *J. Comp. Neurol.* **228**, 432-446.

Table S1. Morphological and functional findings for each cell depicted in Fig. S1

	Cell ID	Days after engraftment (ESGPs)	Days in culture (slice)	Invasion depth	Phenotype
Without I_{KIR}	1	8	16	110 µm	S100β+/GFAP–
	2	10	18	–	–
	3	10	18	60 µm	S100β–/GFAP+
	4	19	31	n.d.	n.d.
With I_{KIR}	5	8	16	–	–
	6	11	21	n.d.	n.d.
	7	13	23	80 µm	S100β+/GFAP+
	8	13	23	–	–
	9	15	25	20 µm	S100β+/GFAP+
	10	16	26	n.d.	n.d.
	11	19	31	n.d.	n.d.
With $I_{K(P)}$	12	6	17	50 µm	S100β–/GFAP+
	13	6	17	60 µm	S100β–/GFAP+
	14	6	14	40 µm	S100β–/GFAP–
	15	6	17	n.d.	n.d.
	16	6	17	n.d.	n.d.
	17	8	16	–	–
	18	8	16	110 µm	S100β+/GFAP–
	19	9	17	60 µm	S100β+/GFAP–
	20	10	18	50 µm	S100β+/GFAP+
	21	10	18	50 µm	S100β+/GFAP–
	22	11	19	–	–
	23	11	18	–	–
	24	11	21	50 µm	S100β+/GFAP+
	25	11	23	n.d.	n.d.
	26	11	23	n.d.	n.d.
	27	13	24	n.d.	n.d.
	28	15	26	n.d.	n.d.
	29	16	27	n.d.	n.d.
	30	17	28	n.d.	n.d.
	31	20	32	n.d.	n.d.

Invasion depth and phenotype were analyzed in a subpopulation of the cells (n.d., not determined; –, specimen lost during tissue processing).